ADVANCES IN ATMOSPHERIC SCIENCES, VOL. 21, NO. 6, 2004, 890–896

A Miniature Robotic Plane Meteorological Sounding System

MA Shuqing[1] (马舒庆), CHEN Hongbin*[2] (陈洪滨), WANG Gai[3] (汪 改),
PAN Yi[3] (潘 毅), and LI Qiang[3] (李 强)

[1] *Atmospheric Observation Experimental Base, China Meteorological Administration, Beijing* 100796

[2] *Institute of Atmospheric Physics, Chinese Academy of Sciences, Beijing* 100029

[3] *Institute of Meteorology Sciences, Meteorology Bureau of Jiangxi Province, Nanchang* 330046

(Received 16 January 2004; revised 12 August 2004)

ABSTRACT

This article presents a miniature robotic plane meteorological sounding system (RPMSS), which consists of three major subsystems: a miniature robotic plane, an air-borne meteorological sounding and flight control system, and a ground-based system. Take-off and landing of the miniature aircraft are guided by radio control, and the flight of the robotic plane along a pre-designed trajectory is automatically piloted by an onboard navigation system. The observed meteorological data as well as all flight information are sent back in real time to the ground, then displayed and recorded by the ground-based computer. The ground-based subsystem can also transmit instructions to the air-borne control subsystem. Good system performance has been demonstrated by more than 300 hours of flight for atmospheric sounding.

Key words: miniature Unmanned Aerial Vehicle, atmospheric sounding, flight test

1. Introduction

The use of aircraft as a meteorological observation platform dates back to the days of World War I. Before the establishment of the radiosonde network, regularly scheduled aircraft observations were conducted in some developed countries, such as the United States. Nowadays, automated weather reports from commercial aircraft have been an important data source for numerical weather prediction models for more than a decade (Moninger et al., 2003). There are still some special aircraft equipped with specific advanced meteorological instruments (sometimes called an aircraft laboratory) for use in atmospheric research campaigns (e.g., Scott et al., 1990; Marenco et al., 1998; Junkermann, 2001).

Besides piloted aircraft soundings, the small model Unmanned Air Vehicle (UAV) has also been employed by some atmospheric investigators to measure atmospheric parameters because of its low cost and high mobility. However, the utility of traditional model UAVs is very limited because they can only fly within sight range under radio control, resulting in a maximum sounding range of about 1 km. Another serious limitation of the model UAV is that there is usually no important location information along with the data. If one wants to equip some ground tracking systems for localization or even navigation, the UAV used would be very big and very heavy, leading to the loss of its flexibility.

The advanced GPS (Global Positioning System) technique makes it possible to develop a new generation UAV-based sounding system. The use of a miniature UAV navigated by GPS for atmospheric sounding was first proposed by Holland et al. (1992). The aircraft called *Aerosonde* was conceived in 1992 and reached operational status in 1995–98. Continuing field operations and development since 1998 led to the *Aerosonde Mark* 3, with approximately 2000 flight hours completed. The paper by Holland et al. (2001) provides an update on the development and operations of the Aerosonde program and expands on the vision for the future, including instrument payloads, observational strategies, and platform capabilities.

At nearly the same time, we began to develop the same kind of atmospheric sounding system by means of an autonomous miniature UAV in 1992–95 and flew the early prototypes in 1996 with funding from the China Meteorological Administration (CMA) (Ma et al., 1997). Since 1997, our UAV sounding system

*E-mail: chb@mail.iap.ac.cn

has taken part in several field experiments, for example, the "SVAT Interaction Observation Campaign over Inner-Mongolia Arid and Semi-arid Region" (IMGRASS) in 1998–2001.

In this paper, we present our robotic plane meteorological sounding system (RPMSS). In section 2, the flight platform based on the model UAV and the corresponding ground-based system are described. In section 3, the description of the air-borne sensors and observational modes is given with an emphasis on a new method for sensor-less wind measurement. In section 4, some sounding results are shown. Finally, a short summary and discussion are given in section 5.

2. Sounding platform and ground-based subsystem

Figure 1 shows a photograph of the miniature plane used as a flying sounding platform. The aerodynamical layout is the combination of conventional and duck type ones. The engine is mounted on the rear end of the plane airframe. The take-off weight is about 13 kg. In order to verify the function of the plane, four test flights were conducted up to the maximum wind speed of 10–12 m s^{-1} in the autumn of 1996. The plane's stability and serviceability were proved to be good. Another demonstration flight was carried out on 18 December 1997. During this test, the flight was completed safely at a wind speed of 18–20 m s^{-1} and the plane flew approximately 40 km away from the command site.

The specification of the plane is as follows:

Wing span: 3.0 m
Wing area: 0.62 m^2
Airscrew diameter: 0.46 m
Take-off weight: about 13 kg
Maximum speed: about 30 m s^{-1}
Maximum climbing ratio: about 3 m s^{-1}
Flight Ceiling: about 5 km
Endurance: 4–8 hr (dependent on payload weight)
Fuel: gasoline
Navigation: GPS.

The schematic diagram of the onboard control system is shown in Fig. 2. The main onboard equipments is

(1) onboard computer,
(2) the conversion circuit,
(3) GPS receiver (location error is about 100 m, leading to a ground speed error of about 0.1 m s^{-1}; it can provide information on the longitude, latitude, altitude, ground velocity, etc.),
(4) the transceiver (adopting common VHF, UHF, or other communication equipment to send information from the modem to the ground),
(5) half duplex modem (maximum baud rate of 1200 bits per second),
(6) servos (to change the flight status) and gyros (to increase stability of the UAV flight),
(7) telemetric receiver for receiving instruction from the ground-based subsystem, and
(8) meteorological sensors for measuring atmospheric temperature, humidity and pressure.

The ground-based subsystem consists of

(1) a transceiver (matched with onboard equipment),

Fig. 1. Photograph of the miniature unmanned air vehicle (UAV).

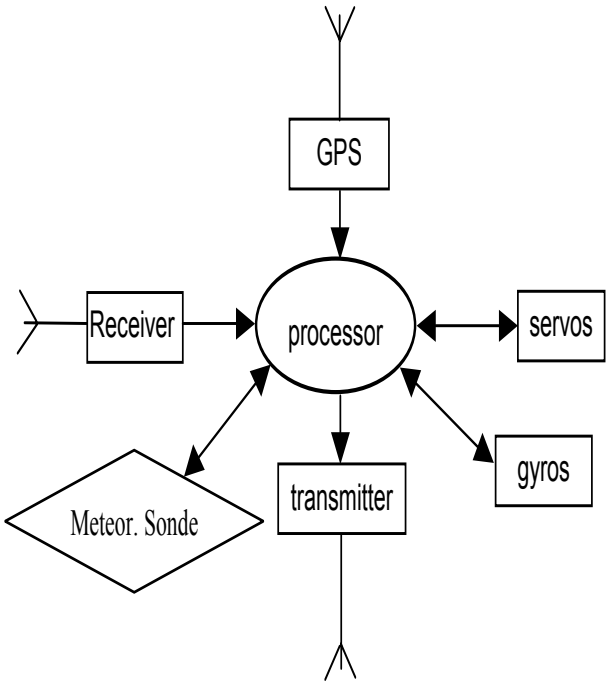

Fig. 2. Schematic diagram of the onboard control and measurement system.

(2) a modem (matched with onboard equipment), and

(3) a micro-computer, used to receive, process, and display the data from the plane; read localization information of the designed flight route and transfer initialization data to the onboard computer before the plane takes off; and dispatch instructions to the onboard computer.

A mini onboard control system was innovatively developed for the UAV atmospheric sounding system. The onboard computer is the brain of the control system, and the GPS receiver is the predominant information source. The reliability of the onboard computer is very important for the control system. The 80C198 single chip CPU is chosen for the onboard computer, which has abundant I/O functions. The peripheral circuit adopts a widely used programmable chip. The onboard computer used has special advantages such as a high integrating degree, small size, and low power consumption. The control system includes both onboard and ground-based equipment.

The onboard computer software function modules include

(1) parameter setting and diagnose module;
(2) GPS information receiving module;
(3) information handling module;
(4) mathematics operation module;
(5) route management module;
(6) servo management module;
(7) sensor information gathering module;
(8) communication module.

In the onboard computer, the software modules run one at a time according to how they are dispatched through intervention and interruption (see left block in Fig. 3). The onboard computer software system is a multitasking one, which increases the complexity of the software system but improves the integration degree and reliability of the hardware and reduces the cost.

Figure 3 shows the flow chart of the automatic control system. The first step is to perform a self-test of the onboard control system after the input of the autonomous flight trajectory data from the ground-based computer. If the self-test completes successfully, no alarm signal is sent to the ground-based computer for surveillance and all modules in the onboard computer start to function in turn. The second step is to initialize all onboard software modules and to acquire the GPS, flight status, and meteorological observation data. The "GPS receiving" intervention module is for receiving and storing the GPS data; the "Tele-command" module is for receiving and storing the tele-command information for adjusting flight status, accelerograph and other parameters; the "servo operation" module is used to control the rudder's operation according to the digitalized command data; and the "dynamical test" module serves to test and manage the procedure of the onboard computer operation. If the system is in the radio-control mode (normally used during take-off and landing) or in tele-command mode (sometimes used in mid flight for adjusting the flight status including flight direction, height, and accelerograph), the UAV flight follows the radio commands from the ground. When the autonomous flight mode switches on, the onboard computer will work out the parameters for the servo-rudder operation based on the current flight status, the received GPS data, and the location of the first (or next) point in the predesigned flight trajectory. For the purpose of safety,

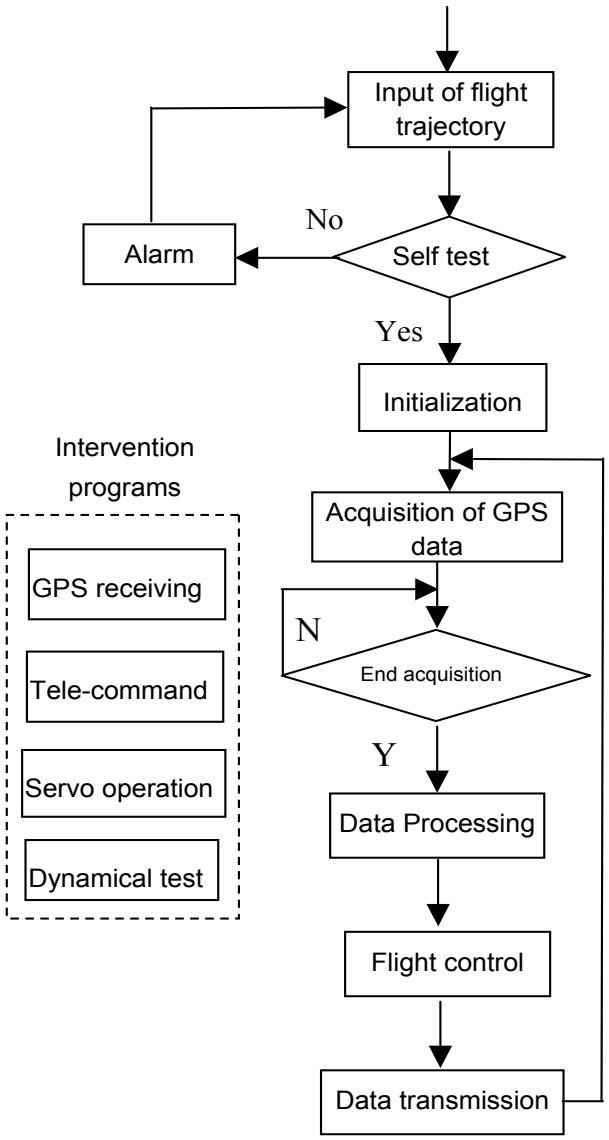

Fig. 3. Flow chart of the automatic flight control system.

Table 1. Main specifications of the meteorological sensors.

Parameter	Measurement range	Accuracy
Temperature (°C)	–90–50	0.3
Relative Humidity (%)	0–100%	5%
Pressure (hPa)	5–1050	0.5

there are limits on the increments for bending, climbing, and descending during the automatic control. And in order to callback the autonomous UAV, the last 4–6 points in the pre-designed flight trajectory are given over the landing site and can be passed through in repetition.

3. Air-borne sounding system and wind velocity measurement

In order to measure the atmospheric parameters, the miniature UAV is equipped with a newly developed digital radiosonde. As a whole, it consists of electronic sensors, measurement circuits and a digital processing unit. Figure 4 shows the frame chart of this digital electronic radiosonde. The temperature, humidity and pressure sensors are mounted on the left or right side of the fuselage of the UAV.

The temperature sensor is a thermal resistance type sensor; the a humidity sensor is a humidity sensitive capacitor; and the pressure sensor is a silicon type one. The measurement ranges and accuracies of the temperature, humidity, and pressure sensors are given in Table 1, all meeting the requirements of meteorological soundings. Measurement and processing are performed by the processing unit composed of a measurement circuit and a single chip computer. The gathered and processed digital data are compiled into the airborne control unit data flow in interception mode and then transmitted to ground receiving system. The use of digital data processing gives the meteorology radiosonde a higher accuracy and makes it less susceptible to interference.

To reduce the payload weight, a new method for measuring wind profiles has been developed. Usually, wind velocity measurement by means of aircraft is conducted by measuring the difference of the airplane air velocity and ground velocity of the aircraft. In this case, sophisticated sensors and processing units are required onboard to obtain the airplane air velocity.

The sensor-less wind velocity observation by the RPMSS is conducted by making a special flight mode, i.e., a plane circular flight mode. This method is based on the fact that the UAV can fly in a stationary circle above the ground if there is no wind, and when this circular flight is shifted by the horizontal air velocity, it becomes a spiral on the ground, as illustrated in Fig. 5. Note that the flight trajectory can always remain as a circular path relative to the stationary wind field.

The method, called the horizontal-velocity-return -zero-method, is detailed in the following. When the plane flies a complete circle by returning to the same point relative to the air, the sum of the horizontal air velocity vector will be zero and the mean horizontal wind velocity is equal to the mean ground velocity of the plane.

The relationship between the air velocity $v_{\rm a}$, ground velocity $v_{\rm g}$ of the plane and wind velocity v is given by

$$v = v_{\rm g} - v_{\rm a} \,. \tag{1}$$

Assuming that the plane flies at a constant speed along a horizontal circle, the longitude and latitude components can be expressed as:

$$\begin{cases} v_{{\rm a}x} = A\cos(\omega t) \,, \\ v_{{\rm a}y} = A\sin(\omega t) \,, \end{cases} \tag{2}$$

where ω is the angular speed, A is the modulus of $v_{\rm a}$. Integrating both sides of Eq. (2) over the time period T of one circular flight, we obtain

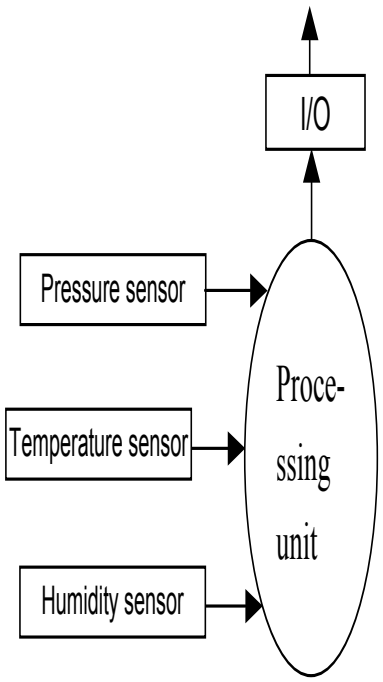

Fig. 4. Diagram of the air-borne electronic sonde for measuring the air temperature, humidity and pressure.

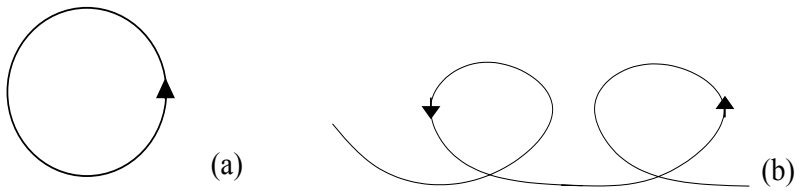

Fig. 5. Ground projection of a circular fight trajectory: (a) zero wind speed and (b) non-zero wind speed.

$$\int_0^T v_{\mathrm{a}x}dt = \int_0^T A\cos(\omega t)dt = 0\ ,$$
$$\int_0^T v_{\mathrm{a}y}dt = \int_0^T A\sin(\omega t)dt = 0\ .$$

Consequently, the integration of both sides of Eq. (1) gives

$$\frac{1}{T}\int_0^T vdt = \frac{1}{T}\int_0^T v_{\mathrm{g}}dt = \overline{v}\ . \tag{3}$$

Thus, the mean horizontal wind velocity $\overline{v}$ is related only to v_{g} in the time period of T. The value of v_{g} is given by means of the onboard GPS receiver once per second, so

$$\overline{v} = \frac{1}{T}\sum_{i=1}^{T} v_{\mathrm{g}i} \quad (i = 1, 2, \ldots, T)\ , \tag{4}$$

where $v_{\mathrm{g}i}$ is the horizontal ground velocity of the ith second obtained from the GPS receiver. If we assume the longitude and latitude coordinates given by the GPS receiver at the ith second to be x_i and y_i, then the components of v_{g} in the x and y directions are

$$\begin{cases} v_{\mathrm{g}xi} = (x_i - x_{i-1}) \\ v_{\mathrm{g}yi} = (y_i - y_{i-1}) \end{cases} \quad (i = 1, 2, 3, \ldots, T)\ . \tag{5}$$

So, the components of horizontal wind velocity v in the x and y directions are

$$\begin{cases} v_x = \dfrac{1}{T}\displaystyle\sum_{i=1}^{T} v_{\mathrm{g}xi} = (x_T - x_0)/T \\ v_y = \dfrac{1}{T}\displaystyle\sum_{i=1}^{T} v_{\mathrm{g}yi} = (y_T - y_0)/T \end{cases} \quad (i = 1, 2, 3, \ldots, T)\ . \tag{6}$$

It can be seen that the measured horizontal wind velocity in this way is theoretically the same as that obtained by the conventional balloon wind measurement method, i.e., the wind speed being derived from the displacement of the balloon or here, the spiral circles flown by the UAV. The test flights have shown that the results obtained by this UAV system possess good accuracy (see Ma et al., 1999).

An analytical method has also been developed to derive wind speed from a segment of the spiral flight trajectory. When the UAV flies in the air along a circle with constant speed, in the ground coordinate framework, the flight track location of the air vehicle can be given by

$$\begin{cases} x = v_{\mathrm{f}x}\cdot t + r\cdot\cos(\omega t + \alpha) + C_x\ , \\ y = v_{\mathrm{f}y}\cdot t + r\cdot\sin(\omega t + \alpha) + C_y\ , \end{cases} \tag{7}$$

where x and y are the ground coordinates of the aircraft, $v_{\mathrm{f}x}$ and $v_{\mathrm{f}y}$ are the components of horizontal wind velocity in the x and y directions, r and ω are the radius and angular speed of the UAV circular fight, α is the initial phase, C_x and C_y are the original coordinates of the circle center. Derivatives of both x and y versus the time t lead to

$$\begin{cases} v_x = dx/dt = v_{\mathrm{f}x} - r\omega\sin(\omega t + \alpha)\ , \\ v_y = dy/dt = v_{\mathrm{f}y} + r\omega\cos(\omega t + \alpha)\ . \end{cases} \tag{8}$$

Equations (8) are nonlinear. In order to obtain analytical expressions, we can expand Eq. (8) into a Taylor series and omit the terms of order two and higher to get

$$\begin{cases} v_x = (v_x) + \dfrac{\partial v_x}{\partial v_{\mathrm{f}x}}\Delta v_{\mathrm{f}x} + \dfrac{\partial v_x}{\partial r}\Delta r + \dfrac{\partial v_x}{\partial \omega}\Delta\omega + \dfrac{\partial v_x}{\partial \alpha}\Delta\alpha \\ v_y = (v_y) + \dfrac{\partial v_y}{\partial v_{\mathrm{f}y}}\Delta v_{\mathrm{f}y} + \dfrac{\partial v_y}{\partial r}\Delta r + \dfrac{\partial v_y}{\partial \omega}\Delta\omega + \dfrac{\partial v_y}{\partial \alpha}\Delta\alpha\ , \end{cases} \tag{9}$$

where (v_x) and (v_y) are the values obtained from Eqs. (8) using the original values $v_{\mathrm{f}x0}, v_{\mathrm{f}y0}, r_0, \omega_0$, and α_0; $\Delta v_{\mathrm{f}x} = v_{\mathrm{f}x} - v_{\mathrm{f}x0}$, $\Delta v_{\mathrm{f}y} = v_{\mathrm{f}y} - v_{\mathrm{f}y0}$, $\Delta r = r - r_0$, $\Delta\omega = \omega - \omega_0$, $\Delta\alpha = \alpha - \alpha_0$. In Eq. (9) there are 5 unknowns: $\Delta v_{\mathrm{f}x}, \Delta v_{\mathrm{f}y}, \Delta r, \Delta\omega$, and $\Delta\alpha$. When N continuous groups of values (v_{xi}, v_{yi}) are obtained from the GPS receiver, there will be $2N$ equations of one order and five elements. In order to eliminate the stochastic error, set $2N > 5$, solve $\Delta v_{\mathrm{f}x}, \Delta v_{\mathrm{f}y}, \Delta r, \Delta\omega$, and $\Delta\alpha$ by using the least squares fitting method, and add them to $v_{\mathrm{f}x0}, v_{\mathrm{f}y0}, r_0, \omega_0, \alpha_0$. Put them into Eq. (9), and a set of equations are obtained again and solved iteratively until $\Delta v_{\mathrm{f}x}, \Delta v_{\mathrm{f}y}, \Delta r, \Delta\omega$, and $\Delta\alpha$ become smaller than the preset criteria values. Then, the wind velocity components $v_{\mathrm{f}x}$ and $v_{\mathrm{f}y}$ are obtained with a certain accuracy.

It is shown in a series of numerical simulations that when $N = 14, 19$, and 24, the standard errors of longitude and latitude components of wind velocity are only about 0.27, 0.11, 0.05 m s^{-1} and 0.24, 0.10, 0.04 m s^{-1} respectively, which is small enough as required.

Comparing the analytical method with the horizontal-velocity-return-zero method, it can be seen that the flight patterns are the same, but in the latter, the wind velocity is calculated by the coordinates of the start and end points of the flight circle; the analytical method needs only N data groups of continuous points without knowing the heading of the aircraft, but much more computing time is required and the method does not provide real time wind velocity.

4. Test soundings and applications

A few sounding test flights were conducted over the new airport of Nanchang City during September to October 1997. Some intercomparison results were given in Ma et al. (1999). It is worth noting that the PRMSS can provide higher spatial resolution of observations and perform horizontal measurements at a nearly constant altitude. Moreover, it takes only about 30 minutes to prepare the system for flight sounding after arriving at an operation site.

In 1998, the RPMSS was used in a field campaign of IMGRASS supported by the Natural Science Foundation of China (NSFC). About 80 profiles of atmospheric pressure, temperature, humidity and wind speed as well as wind direction were obtained from 54 flights. Figure 6 shows an example of the RPMSS measurement results obtained on 26 May 1998. It is seen that in the morning, the UAV entered into cloud layer and the wind speed increased rapidly with height, up to $\sim$17 m s^{-1} at 2400 m, making the RPMSS take a very long time (about 1 hour) to come back; at 1430 LST, the wind was quite strong near the ground with a speed of $\sim$10 m s^{-1} but the vertical shear decreased.

By 2001, a novel ozone sounding system was also developed based on the miniature UAV. The ozone sensor used is the type of ECC (Electrochemical Concentration Cell) with a weight of approximately 400 g. It is shown by several inter-comparison flight experiments that the system performance is very good and the ozone measurement accuracy is similar to that of free-flight balloon ozone sondes. As an example of ozone sounding, Fig. 7 shows three ozone profiles obtained with both tethered balloon and UAV sondes on 1 April 2003 in a southern suburb of Beijing. For comparison, the tethered balloon sonde was launched at the Atmospheric Observation Experimental Base/CMA, and the UAV ozone sonde was conducted about 3 km away. During that day experiment of ozone sounding, the boundary atmosphere with a light haze was quite stable. It is seen from Fig. 7 that the ascent and descent flight measurements are in good agreement with each other and a maximal difference between the UAV and tethered balloon sondes is less than 5 nPa. This implies that the flight climbing state has no considerable effect on the ozone sounding with the miniature UAV.

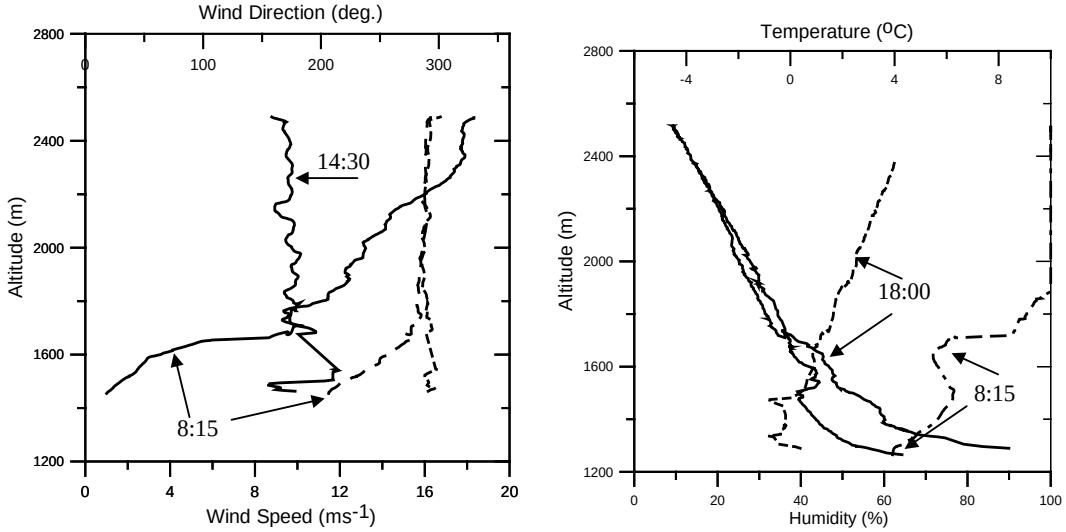

Fig. 6. Profiles of wind (solid for speed and dashed for direction), temperature (solid), and humidity (dashed) measured by the RPMSS on 26 May 1998.

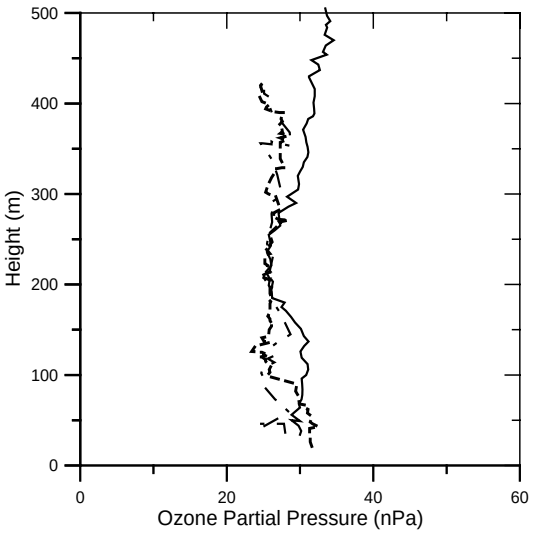

Fig. 7. Intercomparison of the ozone sondes by using a tethered balloon (solid line) and autonomous UAV (short dashed line for ascent flight and dash dotted line for descent) on 1 April 2003 in Beijing.

5. Summary and discussion

The advantages of the robotic plane meteorological sounding system (RPMSS) are its small size, light weight, and high flexibility. Some test and application flights have demonstrated a good system performance, providing atmospheric sounding data with required accuracies from the surface to 5 km of altitude and from the command site to approximately 100 km of horizontal distance. So, it can be widely used in atmospheric sounding and environmental monitoring, especially in remote areas.

The current model of the RPMSS is still in development and many improvements need to be made in the future. For example, the flight endurance and ceiling height can be extended to approximately 20 hours and 10 km respectively if the model UAV is equipped with a more powerful engine, and in this case both long-range and continuous day-to-night atmospheric soundings can be realized; the application of the RPMSS can be broadened if the system integration is improved and the long-range communication problem is resolved.

Acknowledgments. This work was supported by the China Meteorology Administration and the China Natural Natural Science Foundation under Grant Nos. 49975010 and 49790020-6. We would like to thank our colleagues, TAN Qun, ZHAO Yu, FAN Keping, and XUAN Yuejian, for their contributions to the development of the system and to the field experiments.

REFERENCES

Holland, G. J., T. McGeer, and H. Youngren, 1992: Autonomous aerosondes for economical atmospheric soundings anywhere on the globe. *Bull. Amer. Meteor. Soc.*, **73**(12), 1987–1998.

Holland, G. J., and Coauthors, 2001: The Aerosonde robotic aircraft: A new paradigm for environmental observations. *Bull. Amer. Meteor. Soc.*, **82**(5), 889–901.

Junkermann, W., 2001: An ultralight aircraft as platform for research in the lower troposphere: System performance and first results from radiation transfer studies in stratiform aerosol layers and broken cloud conditions. *J. Atmos. Oceanic. Technol.*, **18**, 934–946.

Ma Shuqing, Wang Gai, and Pan Yi, 1997: Preliminary experiments of atmospheric sounding using Mini Unmanned Air Vehicle. *Journal of Nanjing Meteorology Institute*, **20**(2), 171–177. (in Chinese)

Ma Shuqing, Wang Gai, Pan Yi, and Wang Ling, 1999: An analytical method for wind measurement using miniature aircraft. *Chinese J. Atmos. Sci.*, **23**(2), 202–208.

Marenco, A., and Coauthors, 1998: Measurement of ozone and water vapor by airbus in-service aircraft: The MOZAIC airborne program, an overview. *J. Geophys. Res.*, **103**(D19), 25631–25642.

Moninger, W. R., R. D. Mamrosh, and P. M. Pauley, 2003: Automated meteorological reports from commercial aircraft. *Bull. Amer. Meteor. Soc.*, **84**(2), 203–216.

Scott, S. G., T. P. Bui, and K. R. Chan, 1990: The meteorological measurement system on the NASA ER-2 aircraft. *J. Atmos. Oceanic. Technol.*, **7**(4), 525–540.